Repository Istituzionale dei Prodotti della Ricerca del Politecnico di Bari

# Room acoustic modelling of textile materials hung freely in space: from the reverberation chamber to ancient churches

This is a post print of the following article

*Original Citation:*
Room acoustic modelling of textile materials hung freely in space: from the reverberation chamber to ancient churches / Alonso, Alicia; Martellotta, Francesco. - In: JOURNAL OF BUILDING PERFORMANCE SIMULATION. - ISSN 1940-1493. - 9:5(2016), pp. 469-486. [10.1080/19401493.2015.1087594]

*Availability:*
This version is available at http://hdl.handle.net/11589/55666 since: 2021-03-05

*Published version*
DOI:10.1080/19401493.2015.1087594

Publisher:

*Terms of use:*

(Article begins on next page)

12 October 2024

To appear in the *Journal of Building Performance Simulation*
Vol. 9, No. 5, September 2016, 1–21

# *Room acoustic modeling of textile materials hung freely in space: from the reverberation chamber to ancient churches*

Alicia Alonso [a] and Francesco Martellotta*[b]

[a]*Instituto Universitario de Arquitectura y Ciencias de la Construcción – Escuela Técnica Superior de Arquitectura, Universidad de Sevilla, Seville, Spain*;
[b]*Dipartimento di Scienze dell'Ingegneria Civile e dell'Architettura, Politecnico di Bari, Bari, Italy*

(*Received 00 Month 20XX; final version received 00 Month 20XX*)

The aim of this study is to investigate how sound absorbing materials like curtains should be modeled in geometrical acoustic software when hung freely in space. The use of these tools is widespread today. Whatever the scope of the simulation, dealing with textile materials can be particularly challenging as they both absorb and transmit sound, and absorption is dependent on distance the walls. Therefore, care must be taken to enter properly validated data. Absorption coefficients found in the literature are measured with samples close to wall, and are not suitable when materials are hung freely. The effects of material placement on both absorption and transmission coefficients were therefore investigated using scaled-down physical models of a reverberant chamber and a church. Subsequently, geometrical acoustic models of both spaces were used to demonstrate that simulated results are reliable assuming that absorption and transmission coefficients are correctly determined.

Post-print version, please download editorial version at DOI: 10.1080/19401493.2015.1087594

**Keywords:** acoustic simulation; sound absorption; textile materials; church acoustics.

## 1. Introduction

At present, acoustic modeling of space, either to support a new design or to revive an ancient building that is no longer available in its original condition, can be carried out, with limited effort, using one of the many geometrical acoustic simulation tools available. These tools are based on variations of the well-known ray tracing algorithm (Vorlander 2008) and require a sufficiently accurate geometrical model of the space and a proper knowledge of the acoustic properties of the surfaces, including absorption, scattering and, when applicable, transmission coefficients. The geometrical part of the task is usually quite simple, as the level of detail required by the model is relatively low and, conversely, an abundance of small details may cause longer calculations with little impact on the accuracy of the final results. In addition, the choice of material properties is much more delicate, and can often have substantial impact on the final results. The literature provides a wealth of information about the sound absorption of many types of materials (Cox and D'Antonio 2004), but when scattering and diffusion are taken into account the amount of information is noticeably reduced and prompts a return to "educated guessing" based on experience as the sole rule. Small differences in the way different software handle scattering also contribute to further complicating this task. A more rigorous approach to modeling these phenomena can be based on the numerical solution of the wave equation. Finite elements (FEM) and finite difference time domain (FDTD) methods are gaining increasing attention as they allow a straightforward inclusion of boundary effects, capable of accounting for absorption/transmission/reflection, as well as

*Corresponding author. Email: francesco.martellotta@poliba.it

Figure 1. Typical arrangement of tapestries hung between the naves of the Cathedral of Cologne.

edge diffraction. Unfortunately these methods require a huge computational load and are therefore limited to smaller spaces and low frequency domain.

However, the aim of this paper is to address a very specific problem that arose while investigating the effect of ephemeral architecture on the acoustics of ancient churches (Alonso et al. 2014). The problem is that of establishing the best way to model textile materials hung free in space. Textiles are porous sound absorbing materials whose properties are well known and understood (Cox and D'Antonio 2004; Kuttruff 2009). However, although their theoretical behavior can be predicted with relative ease, most of the experimental data refer to materials close to walls, or draped, with very little information available on textiles hung freely in space (Ognedal 2005). Under these conditions not only does sound absorption change depending on wall placement (Martellotta and Castiglione 2011), but sound transmission through the panel can also play an important role, particularly when the material divides the same space into parts.

A typical case of this is that of ancient churches in which the space was richly decorated for major festive celebrations using various kinds of textiles, with different arrangements (Goehring 2009). Draperies, embroideries or veils were attached to walls or columns (Figure 1), while coverings were reserved for altarpieces, shrines and tombs. Materials and their arrangement could vary significantly depending on the church, event, or time period, as can be deduced from text descriptions, iconographic material, inventory accounts or examples that have been preserved (Weigert 2004; Santos-Gomez and San Andres-Moya 2004). Iconographic material and some samples preserved in the cathedral of Seville show that velvet draperies were hung from the columns and walls. In other churches, such Saint Petronio Basilica in Bologna (Schnoebelen 1969), pieces of damask used in main celebrations were generally hung and draped on the arches and on the vaults. During Easter celebrations in many Spanish churches and cathedrals, the altarpieces were covered with a light cloth or hanging curtains, which were sometimes placed at the entrances to the side chapels. In the cathedral of Seville, there are still marks on the walls which confirm this practice in the past. In any case, without going back so far in time, freely hung materials can be found in every stage-house in theaters as part of the scenery, and in many auditoria and concert halls they serve as a means to control reverberation time. Consequently, as the acoustic implications deriving from the widespread use of such materials may be significant, understanding how to handle them in computer simulations, particularly in those cases where no on-site calibration measurement is possible, becomes of primary importance to avoid unrealistic results.

Considering the importance of validating the results of computer simulations against real-world data, and the difficulty of applying large amounts of textile materials to real spaces, the use of scale models was considered as a possible alternative. This technique, mostly developed when computer simulation was not a viable option (Barron 1983), is based on the assumption that in a 1:N scaled-down model of the space, sound waves N-times smaller (i.e. with a frequency N-times higher)

propagate like usual sound waves in real spaces. From a geometrical perspective this approach is very effective and, in fact, it is used when complex wave-based phenomena are involved (Farnetani et al. 2008; Ryu and Jeon 2008), as well as in order to validate theoretical models or numerical simulation techniques (Chiles 2004; Summers et al. 2005; Luizard, Polack, and Katz 2014). In addition, the method has been often used in building acoustics to investigate sound insulation properties of materials (Astolfi et al. 2000; Simons 1982). However, reproduction of real-scale acoustic properties is far from simple and often requires several attempts and a certain degree of adaptation.

In this case, the problem of adaptation was limited somewhat as scale models were used as reference (albeit as realistic as possible) to understand how the absorption and transmission coefficients of textile materials could be modeled in computer simulation tools based on geometrical acoustics. To do so, acoustic properties of real-scale textile materials are first discussed in reference to theoretical models and to data available in the literature in order to identify the characteristics that scaled-down materials should possess. Subsequently, the methods and results of material characterization in scaled-down models are presented. Measurements are first carried out in a 1:20 reverberation room and validated against a geometrical acoustic model. Selected materials are then applied to a 1:20 church model to investigate their effect in a larger space, where they divide the nave from the side aisles. Again, geometrical acoustic models of the same space are employed to validate the use of the material properties measured earlier. To conclude, a brief comment is made on the possible effects of textiles on church acoustics.

## 2. Acoustic properties of textile materials

The acoustic behavior of materials is commonly described in practice by means of absorption ($\alpha$) and transmission ($\tau$) coefficients. The former is defined as the ratio of the absorbed to the incident acoustic energy, while the latter is the ratio of the transmitted to the incident acoustic energy, more frequently found in the form of sound reduction index $R$ (or transmission loss), defined as $R = 10\log(\tau^{-1})$. To avoid misunderstandings, it should be specified that in room acoustics the transmitted energy is usually of no interest (as it goes into a different room), and thus it is included in the amount of energy actually dissipated inside the material (i.e. $\alpha$ is actually the sum of dissipated and transmitted energy fractions). However, when dealing with materials that are not boundaries of the room, the energy transmitted remains in the same space, making it important to address coefficients correctly. Both $\alpha$ and $\tau$ are frequency dependent and may refer to normal incidence or, more frequently, to a diffuse field.

As soon as a more detailed analysis of the theory behind acoustic properties of materials is undertaken, the role of characteristic impedance $Z$ of the surface appears. This parameter is given by the ratio between pressure and particle velocity at the boundary of the surface and, is most generally a complex number, meaning that it affects both their amplitude and phase. A derivation of the relations between $Z$ and $\alpha$ is beyond the scope of the paper and can be found in one of the many textbooks on the topic (Cox and D'Antonio 2004; Kuttruff 2009). However, when $Z$ is very similar to air impedance $Z_0 = \rho c$ (where $\rho$ is the density and $c$ is sound speed), $\alpha$ obtains the highest value, while when $Z$ is much larger the surface is rigid and $\alpha$ tends to zero.

Textile materials, usually in the form of curtains or drapes, are essentially thin porous absorbers which dissipate acoustic energy due to friction inside pores. As such, their characteristic impedance, can be expressed by means of models based on purely empirical approaches (Delany and Bazley 1970), or on semi-analytical phenomenological models (Allard and Champoux 1992). In the first case $Z$ is a complex function of flow resistivity ($\sigma$), which is a measure of how easily air can enter the pores and the resistance encountered throughout its structure:

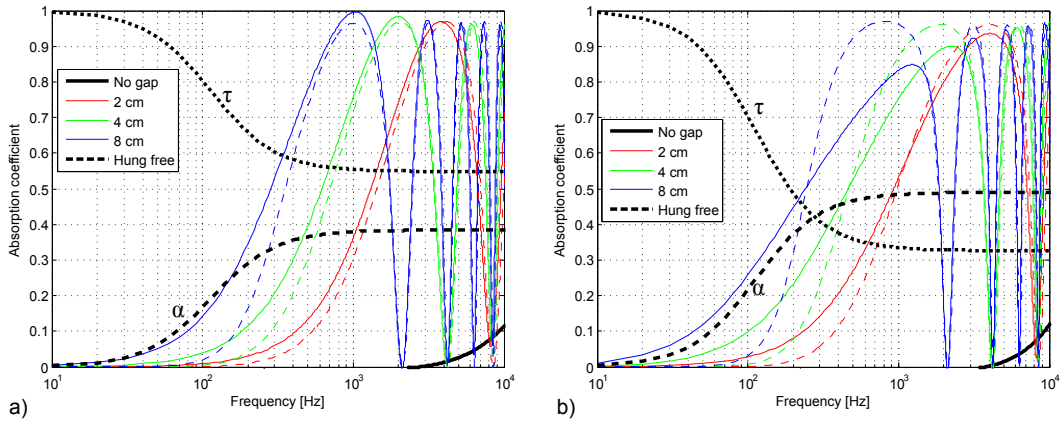


Figure 2. Normal incidence absorption coefficients for a 1 mm layer of porous textile as a function of different distances from a rigid wall. Dashed lines correspond to the simplified model for thin layers, while solid lines correspond to Delany and Bazley model. Thick dashed and dotted lines correspond to dissipation and transmission coefficients for samples hung freely calculated according to thin layer model (Kuttruff 2009). a) $m = 300g/m^2$, $\sigma_s = 280Pa \cdot s/m$; b) $m = 500g/m^2$, $\sigma_s = 600Pa \cdot s/m$)

$$\sigma = \frac{\Delta p}{vd},$$

where $\Delta p$ is the pressure drop that occurs between the faces of the material, $v$ is the flow velocity, and $d$ is the material thickness. The ratio between $\Delta p$ and $v$ is referred to as flow resistance ($\sigma_s$), and consequently $\sigma_s = \sigma d$. Phenomenological models are much more complex as they depend on many other material properties, but their discussion is beyond the scope of this study. For very thin layers of porous absorbers, like curtains, it can be observed (Kuttruff 2009) that when the fabric has a finite mass and vibrates as a whole, characteristic impedance can be expressed as a simple function of flow resistance and surface mass ($m$):

$$Z_r = \left(\frac{1}{\sigma_s} + \frac{1}{j\omega m}\right)^{-1}.$$

However, in the case of curtains and textiles, the largest contribution to sound absorption derives from the air gap between the material and the rigid wall behind it. In fact, as absorption is due to friction and friction increases with particle velocity, a thin absorbing layer is largely ineffective when is backed by a rigid wall, as particle velocity is zero on its surface. Conversely, as the particle velocity reaches a maximum at a quarter wavelength from the wall, a curtain, though thin, can nonetheless show a better performance, at least at frequencies whose wavelengths are sub-multiples of four times the air gap thickness. Without expounding on the theoretical details of the models, clearly discussed in the books mentioned above (to which the reader is directed for a more thorough understanding of the background), Figure 2 shows a comparison of normal incidence absorption coefficients for typical 1 mm thick lightweight curtains (having different surface mass and flow resistance) as a function of different distances from the wall, predicted following the Delany and Bazley model and the simplified model for thin layers. The difference between the two models is significant only in the low frequency range, where both models are known to be less accurate. When the sample is in front of a hard wall the sound absorption is nearly zero up to 2 kHz, when it shows a mild increase up to 0.1 at 10 kHz. However, as soon as the distance from the rigid wall increases, significant absorption peaks appear and move to lower frequencies, becoming increasingly frequent as the distance grows.

Finally, when the curtain is hung freely in space (sufficiently far from any other wall), it is no

longer a boundary of the room, and therefore the energy transmitted through it is not lost but remains in the room. Under these conditions the absorption coefficient should be better addressed as "dissipation coefficient" to remark it no longer includes the transmitted part. However, for the sake of simplicity, the "absorption" term will be used throughout the paper. Its behavior as a function of frequency shows a smooth growth, remaining substantially flat above a certain frequency. A theoretical limit of 0.5 is found when $Z = 2Z_0$. It is worth noting that when a curtain is hung freely in space both faces contribute to absorption, and therefore in practice the absorber area is doubled. Under these conditions the transmission coefficient can also be calculated and it shows a trend opposite to that of absorption. It starts with high values at low frequencies and smoothly decreases up to a plateau at high frequencies. The latter value is higher when the flow resistance is lower.

When the angle of incidence of sound becomes $\theta$, the above considerations need to be applied only to the components in normal direction to the surface. As the projection of the wavelength in this direction becomes $\lambda/\cos\theta$, (among other effects) this causes the quarter wavelength rule to be applied to higher frequencies as the angle grows. At the same time, sound absorption is lowered. Therefore, when the total average is calculated for all the angles the differences between peaks and valleys are considerably evened out (Fig. 3). For the hung panel the diffuse field value for $\alpha$ is also slightly lower than the normal incidence value, while $\tau$ is higher. It is interesting to observe that when octave bands values are calculated (by averaging over the frequencies of interest), peaks appear only at the lowest frequency corresponding to the $\lambda/4$ rule, while at higher frequencies the values are substantially evened out. The comparison between values for hung free panels and those close to walls suggests that, particularly for resistive materials, the doubling of the absorbing surface for the former may well compensate for the lower absorption. Thus, a textile hung freely might present a higher absorption than the same panel hung straight close to a wall, particularly at higher frequencies. A well known means of increasing sound absorption when using curtains is draping. In fact, drapes determine a variation of the distance from the rigid backing that causes a smoother distribution of the "peaks" over a larger frequency interval. Depending on the fullness of the drape, increased resistance may be obtained resulting in generally higher absorption coefficients. However, predicting such behavior is rarely feasible due to the random nature of drapes.

Following this outline of the theoretical behavior of textiles, we encounter the problem of finding data for use in geometrical acoustic (GA) modeling. Analysis of the data available in the literature (Cox and D'Antonio 2004) shows significant variations depending on density, mount, and percentage of draping. In addition, it is hard to find all the possible configurations for a given type of textile. Values of $\alpha$ and $\tau$ for curtains hung freely are even more difficult to find (Ognedal 2005). Numerically determining them using the approaches outlined above is a possibility, although in this case density and flow resistance must be known (and this is not always the case). Therefore, the only viable option for carrying out a study on the best way to model textiles in GA models, thus analyzing their effect on room acoustics, is to measure all the necessary coefficients. Given that this task was carried out using scale models to realistically represent real rooms, it is advisable to provide the reader with some "reference" values for different types of real-scale curtains for comparison purposes with the subsequent values. These values are given in Table 1, together with measured (or estimated) transmission coefficients.

## 3. Methods

In this work, acoustic measurements were carried out in 1:20 scale models only. A reverberant chamber and a basilica plan church were used to investigate different geometrical configurations and dimensions. Absorption and transmission coefficients of textile materials had to be measured in scaled-down facilities, carefully choosing the materials that could better approximate real-scale behavior. Finally, GA models of both the reverberant chamber and of the church were built using CATT Acoustics (Dalenbäck 2011), and calibrated in order to compare the results against scale

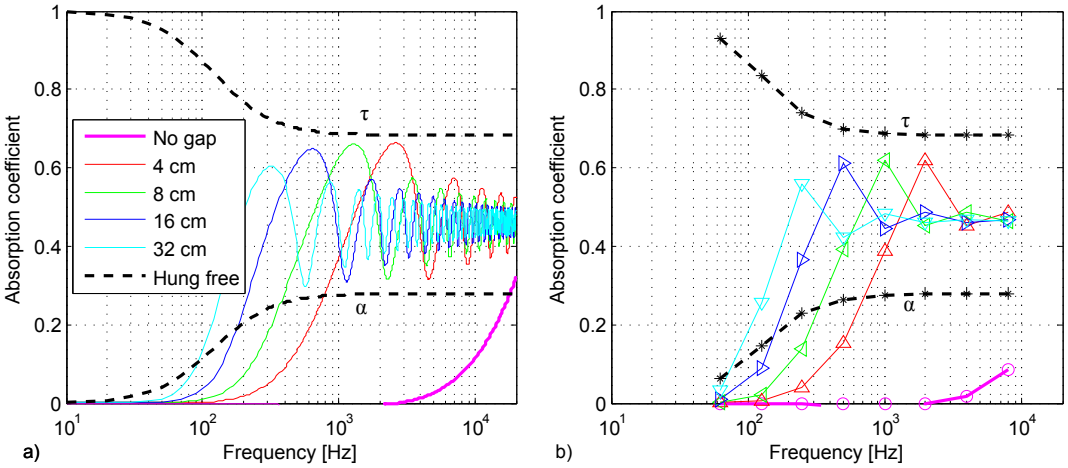


Figure 3. Diffuse field absorption coefficients for a 1 mm layer of porous textile ($m = 300g/m^2$, $\sigma_s = 280Pa \cdot s/m$) as a function of different distances from a rigid wall, calculated according to the simplified model for thin layers. Thick dashed lines correspond to dissipation and transmission coefficients for samples hung freely calculated according to the same model (Kuttruff 2009). Right panel shows the same results averaged over octave bands.

Table 1. Summary of absorption and transmission coefficients as a function of frequency, for textiles taken as reference. For samples hung free, the absorption coefficient is calculated with reference to both faces of the sample.

| ID | Description | Mount | Param. | 125 Hz | 250 Hz | 500 Hz | 1000 Hz |
|---|---|---|---|---|---|---|---|
| R1 | Light tapestry[a], m=200 g/m$^2$ | Straight at 7 cm from wall | $\alpha$ | 0.09 | 0.15 | 0.29 | 0.50 |
| | ($\sigma_s$=200 Pa· s/m) | hung free | $\alpha$ | 0.11 | 0.11 | 0.16 | 0.21 |
| | | | $\tau$* | 0.88 | 0.80 | 0.77 | 0.75 |
| R2 | Velour[b], m=545 g/m$^2$ | hung free | $\alpha$ | 0.08 | 0.19 | 0.33 | 0.42 |
| | ($\sigma_s$=1525 Pa.s/m) | | $\tau$ | 0.63 | 0.51 | 0.33 | 0.25 |
| R3 | M1 Wool serge[b], m=650 g/m$^2$ | hung free | $\alpha$ | 0.11 | 0.24 | 0.36 | 0.43 |
| | ($\sigma_s$=721 Pa.s/m) | | $\tau$ | 0.58 | 0.55 | 0.41 | 0.37 |
| R4 | Heavy velour[c], m=610 g/m$^2$ | hung straight | $\alpha$ | 0.08 | 0.12 | 0.35 | 0.48 |
| | | draped | $\alpha$ | 0.14 | 0.35 | 0.55 | 0.77 |

[a]From Martellotta and Castiglione (2011); [b]Experimental values from Ognedal (2005); [c]From Cox and D'Antonio (2004)

* $\tau$ coefficients calculated according to physical properties.

model measurements.

### 3.1. *Scale models*

Two 1:20 scale models of a reverberant chamber (RC) and of a basilica plan church (CH) were used in order to validate the use of textiles hung freely in GA models under very different geometrical conditions.

The RC model (Fig. 4a) was made of 10 mm thick methacrylate, so that long reverberation was achieved. It had a volume of 208 m$^3$ (full scale) and the shape replicated the chamber of the Politecnico di Bari which complies with ISO 354 (2003) specifications for absorption coefficient measurements. In order to improve diffusion in the RC model, additional polyethylene sheets scattering panels were included in the room. The room-averaged reverberation times (T20) in the octave bands from 125 Hz to 1000 Hz were 4.18 s, 3.25 s, 2.70 s, and 2.17 s respectively.

The CH model (Fig. 4b) was built using only two types of materials: 4 mm thick methacrylate for curved vaults and domes, and 14 mm thick medium density fiberboard (MDF) for the other surfaces. MDF walls were also treated with several layers of a transparent coating in order to reduce sound absorption. The length of the central nave was over 2 m, and the height to the highest point of the dome was 1.5 m, corresponding to a full scale volume of about 18000 m$^3$. Reverberation

Table 2. Measured values in church model (average of two rotated positions of tetrahedron sound source) of the acoustical parameters, spatially averaged for each frequency

| | 125 Hz | 250 Hz | 500 Hz | 1000 Hz | mid |
|---|---|---|---|---|---|
| T20 [s] | 8.92 | 8.38 | 6.75 | 5.23 | 5.99 |
| EDT [s] | 8.77 | 8.17 | 6.56 | 5.38 | 5.97 |
| Ts [ms] | 630 | 588 | 471 | 397 | 434 |
| C80 [dB] | -8.6 | -9.5 | -7.9 | -6.6 | -7.2 |
| D50 [%] | 9.8 | 9.0 | 12.6 | 17.7 | 15.1 |

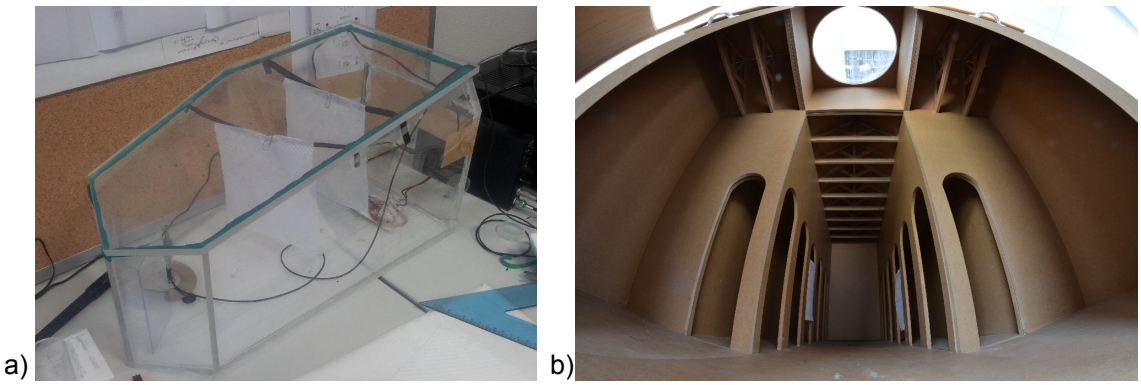


Figure 4. Photographs of the reverberant chamber (a) and church (b) models used in this paper.

time and other acoustic parameters are included in Table 2 and are in good agreement with typical values found in churches of similar shape and volume under unoccupied conditions.

Two positions of the sound source were considered for each scale model. Seven receiver positions were chosen in the RC model, and twelve points were distributed throughout the central nave, aisles and transept of the CH model (Figure 5).

### 3.2. *Measurements of room acoustic parameters*

In order to perform measurements of reverberation time and other room acoustic parameters, a 1/8" GRAS 40 DP microphone was used as the receiver. The transducer had a flat frequency response (within ±1 dB) up to 30kHz and was connected to an Echo Audio-Fire sound card with a sampling frequency of 96 kHz. This sampling frequency ensured measuring signals with a 48 kHz frequency range, which corresponded to a frequency of 2400 Hz in full scale. Beyond that limit air absorption issues became difficult to handle numerically (see below for details). Consequently, the analysis was focused on the full-scale octave bands from 125 Hz to 1000 Hz corresponding to 2.5, 5, 10, and 20 kHz in the scale model. A tetrahedron sound source with three small loudspeakers (one on each side except in the base which lay on the floor) was used as an approximation of an omnidirectional source. In fact, as demonstrated by Leishman et al. (2006), despite this regular polyhedron having a low cutoff frequency, which according to the physical dimensions is 166 Hz (full scale), it shows the most uniform radiation above that limit. Measurements along the horizontal plane in free field conditions showed that small variations (within ±1.5 dB) in level appeared at 250 Hz and 500 Hz octaves (full scale), while at 125 Hz and 1 kHz variations were greater (within ±3.5 dB). In order to reduce directivity effects, which might affect early/late ratios as described by Martellotta (2013), all results were averaged over two measurements resulting from rotating the source 60°. Despite these limits, an electro-acoustic source was preferred over a spark generator as the latter proved unable to offer sufficient signal to noise ratio in the larger church model. Measurements and post-processing were controlled by a MATLAB graphic user interface. Impulse responses (IRs) were obtained through the deconvolution of a 9 s linear sine sweep used as signal.

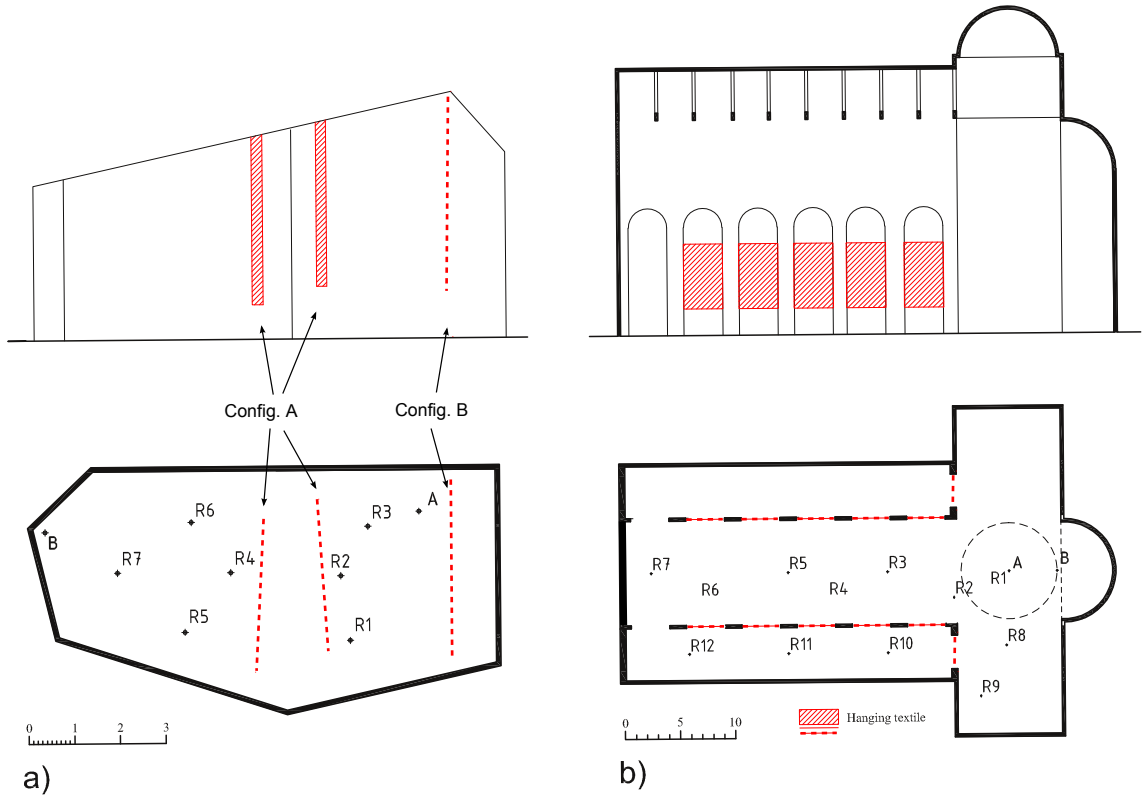


Figure 5. Plans and cross-sections of the reverberant chamber (a) and church (b) models used in this paper. Position of sources (A,B) and receivers (R1-R12) are shown in the plans. Red dashed lines correspond to position of textile samples inside each model. Scale refers to full-scale measurements

A linear rather than exponential sweep was preferred in order to improve signal to noise (S/N) ratio in the high frequency range and allow proper compensation of air absorption effects (Hak et al. 2012).

In fact, air absorption is an important issue to deal with when working with scale models. At higher frequencies, air absorption is considerably greater than the corresponding value referring to the full scale (Wenmaekers et al. 2014). However, as the distance traveled by sound waves is proportionally smaller in scale models, the differences are not as noticeable as the absorption variation might suggest. A possible suitable approach to obtain reliable impulse responses where excess attenuation due to air absorption is removed, is to numerically correct them by estimating air absorption coefficients at different frequencies following ISO 9613 (1993) as a function of air temperature and relative humidity and applying the procedure explained by Wenmaekers et al. (2014). To prevent the noise floor from receiving an unwanted amplification that hampers use of the IR, each impulse response was band filtered beforehand (in one-third octave bands), the noise floor was identified and the correction was then applied in the time domain taking into account only the decaying part of the IR. By using linear sine sweeps the S/N ratio after air absorption compensation was high throughout the spectrum. In the reverberant chamber it spanned from about 75 dB at low frequencies to about 55 dB at 1.25 kHz. In the church, smaller ranges were observed, with a maximum usually above 50 dB (at low frequencies) and a minimum of 35 dB (at 1.25 kHz). After the numerical correction, all the measurements were referred to 20°C and 50% RH, regardless of the original temperature and relative humidity values, which were constantly monitored inside and outside the models. In the end all the relevant monaural room acoustic parameters were calculated according to ISO 3382-1 (2009). Given the standard requirements in terms of S/N ratio for calculating reverberation time, and the ranges observed in the church model only T20 values (based on a 20 dB decay) were considered in order to have coherent values over the whole set of data.

### 3.3. *Acoustic characterization of textile materials for use in scale models*

The measurement of sound absorption coefficients was carried out in the RC model following ISO 354 (2003). The process consisted in measuring reverberation times before and after placing the sample of the material under test inside the RC model. The standard suggests compensating for temperature and humidity variations between the two measurements. However, according to the procedure explained above, after air absorption compensation, all the measured IRs were referred to the same standard conditions, and this correction could be neglected. In any case, in order to further limit the influence of the air absorption on the measurement, the reference reverberation time was redetermined every time a new material was tested (so that temperature and relative humidity variations were largely negligible). In fact, under these conditions absorption coefficients measured with and without air absorption compensation substantially gave the same results. All the $\alpha$ were calculated in 1/3 octave bands over at least 14 different source-receiver combinations, and then averaged, when required, to yield octave bands values.

As already stated, the effect of sound transmission through textiles was one of the key features that the study aimed to investigate. The diffuse field sound transmission coefficient was consequently measured according to ISO 10140-2 (2010). The transmission suite was made of two coupled scaled-down reverberant chambers. The first was that described above, while the second was identical in shape but made of MDF (and therefore less reverberant). The two rooms were divided by a multi-layer structure including two independent 13 mm MDF pieces, separated by a 5 mm rubber mat, located along the perimeter of the 9 $m^2$ (full scale) opening, where the test samples could be placed. All the joins were carefully sealed with modeling clay to prevent unwanted sound leakage. Transmission coefficients were derived from differences in sound pressure levels measured in at least 10 different source-receiver combinations in each room and properly corrected to account for sound absorption in the receiving room as resulting from reverberation time measurements. A 20 s white noise was used as an excitation signal.

Finally, flow resistance was also measured, as it was shown to be a determining parameter for porous materials, and knowledge of it could contribute to better understanding their acoustic behavior. As the standardized method (ISO 1991) could not be implemented easily, the simplified approach proposed by Ingard and Dear (1985) was adopted. This procedure is based on acoustic waves and, consequently, may be less robust than the standardized method. However, as demonstrated by del Rey et al. (2013), for thin and scarcely resistive samples like those under investigation the method proved to be sufficiently accurate. The measurement set up consisted of a 5 mm thick methacrylate tube, with a 40 mm inner diameter. The tube was made up of two parts, each 85 cm long. At one end there was a sound source and at the other a rigid termination, and the test sample was mounted in between. Two microphones were placed in front of the sample and of the rigid termination and properly calibrated in amplitude and phase. Finally, flow resistance was extrapolated by proper processing of the transfer function between the two microphones excited using an exponential sine sweep.

### 3.4. *Geometrical acoustic modeling*

Geometrical acoustic models of both spaces were built to compare the results with those obtained from measurements. Considering the simplified geometry (Fig. 5), the creation of the virtual models was fairly straightforward, not requiring the usual process of simplification and elimination of small (and acoustically negligible) details. Consequently, the most important task was the assignment of surface properties to ensure a good match between simulations and measurements. However, given that each model was made mostly of the same material (methacrylate for RC, MDF for CH), this task was also relatively simple. The acoustic simulations were carried out with CATT Acoustic software v9.0a, using TUCT v1.0 engine (Dalenbäck 2011). As both rooms were closed, had a mixing geometry, and most surfaces had low scattering coefficients, the "basic" algorithm was used. In this case first order reflections are always treated deterministically, meaning that

each ray is split into a part that is reflected according to the laws of geometrical acoustics and one that is scattered. Conversely, higher order reflections are not split, but are treated randomly depending on the scattering coefficient of the surface (e.g. if the latter is 0.1, nine reflection out of 10 will be reflected specularly, while the remaining will be reflected randomly). For the CH model the number of rays was set manually from the minimum suggested by the software (equal to 56,708), up to 100,000 in order to ensure that a sufficient number of rays could enter the side aisles. However, no significant difference appeared in the results, confirming that the minimum value already represented a good choice. The impulse response duration was set coherently with the measured values of T20 in the scale model. For the RC model, the simulation task was less critical because of the smaller volume. However, as the suspended materials samples could create subdivisions, the number of rays used was 50,000 (also greater than the minimum suggested by the software equal to 29,943).

Even though many researchers are now investigating more refined techniques to optimize the calibration task (Pelzer and Vorländer 2013; Christensen et al. 2014), in our case there was only one unknown material at a time, so a more conventional approach was followed. At first, only values of reverberation time were considered in the calibration process, adjusting absorption coefficients derived from measurements (by reverting Sabine's formula) until simulated values differed by less than one just noticeable difference (JND), which corresponds to 5% of the reference value of reverberation time, as defined in ISO 3382-1 (2009). Then, the remaining monaural acoustic parameters were considered in the calibration process of the CH model, assuming as JND values those specified in ISO 3382-1 and those determined for more reverberant spaces like churches, where the subjective threshold perception can differ (Martellotta 2010). In particular, for EDT and D50 the standard values were used (equal to 5% of reference value, and to 5% in absolute value respectively), while for C80 and Ts the alternate values were used (respectively equal to 1.5 dB, and 8.5% of reference value). At this point if the other parameters showed systematic differences from measurements that could be corrected by acting on absorption coefficients they were further modified, trying to limit adverse effects on T20. Otherwise, as these parameters show a marked dependence on source-receiver position, they were mostly used to check for small inaccuracies in source and receiver placement, as well as for trial-and-error adjustment of scattering coefficients of smaller elements.

Considering that most of the surfaces in both models were flat and large (including the samples of textile materials), scattering coefficients were given relatively low values. Recommended values in such cases are equal to 0.10 at all frequencies (Dalenbäck 2011), and the authors' experience confirmed the suitability of such values. Conversely, smaller surfaces such as pillars and trusses were given higher scattering coefficients (variable between 0.7 and 0.9 depending on frequency and obstacle dimensions), also to include diffraction effects at borders. For textile materials scattering coefficients played a minor role, as the amount of energy reflected was much smaller than the amount absorbed and transmitted. Consequently values were assigned for flat surfaces. It is important to point out that for objects having exposed edges CATT allows the user to select an "automatic edge diffusion" option, according to which reflections falling within a quarter wavelength from edges are systematically treated as diffuse to approximate the effect of diffraction. However, in the present case, this option was not used for textiles because two of their edges are adjacent to columns. In addition, as the reflected energy is small, even for the remaining exposed edges the effect was likely to be negligible.

Measured transmission coefficients ($\tau_{\mathrm{M}}$) were used directly (without calibration) to assign "transparency" coefficients ($\tau_{\mathrm{C}}$) in CATT. However, the software handles transmission in a rather peculiar way. In fact, if the surface absorbs $\alpha_{\mathrm{C}}$, the transmitted energy is assumed to be $(1-\alpha_{\mathrm{C}})\tau_{\mathrm{C}}$, and the reflection takes the remaining energy $(1-\alpha_{\mathrm{C}})(1-\tau_{\mathrm{C}})$. Thus, the CATT transparency coefficients are given as a fraction of the energy that is not absorbed rather than of the incident energy. This implied that to use measured transmission coefficient in CATT they first had be converted into $\tau_{\mathrm{C}}$ values according to the formula: $\tau_{\mathrm{C}} = \tau_{\mathrm{M}}/(1-\alpha_{\mathrm{C}})$.

Average absorption coefficients derived from measurements ($\alpha_{\mathrm{M}}$) were, from 125 Hz to 1 kHz,

Table 3. Measured ($T20_M$) and simulated values ($T20_C$) of reverberation time after calibration in each model under reference conditions, spatially averaged for each frequency. Absolute differences between measured and simulated values are given in terms of JNDs.

| Model | Parameter | 125 Hz | 250 Hz | 500 Hz | 1000 Hz | mid |
|---|---|---|---|---|---|---|
| RC | $T20_M$ [s] | 4.18 | 3.25 | 2.70 | 2.17 | 2.49 |
| | $T20_C$ [s] | 4.25 | 3.24 | 2.70 | 2.15 | 2.43 |
| | JND | 0.3 | 0.2 | 0.1 | 0.2 | 0.5 |
| CH | $T20_M$ [s] | 8.92 | 8.38 | 6.75 | 5.23 | 5.99 |
| | $T20_C$ [s] | 8.90 | 8.32 | 6.83 | 5.13 | 5.93 |
| | JND | 0.4 | 0.4 | 0.4 | 0.5 | 0.2 |

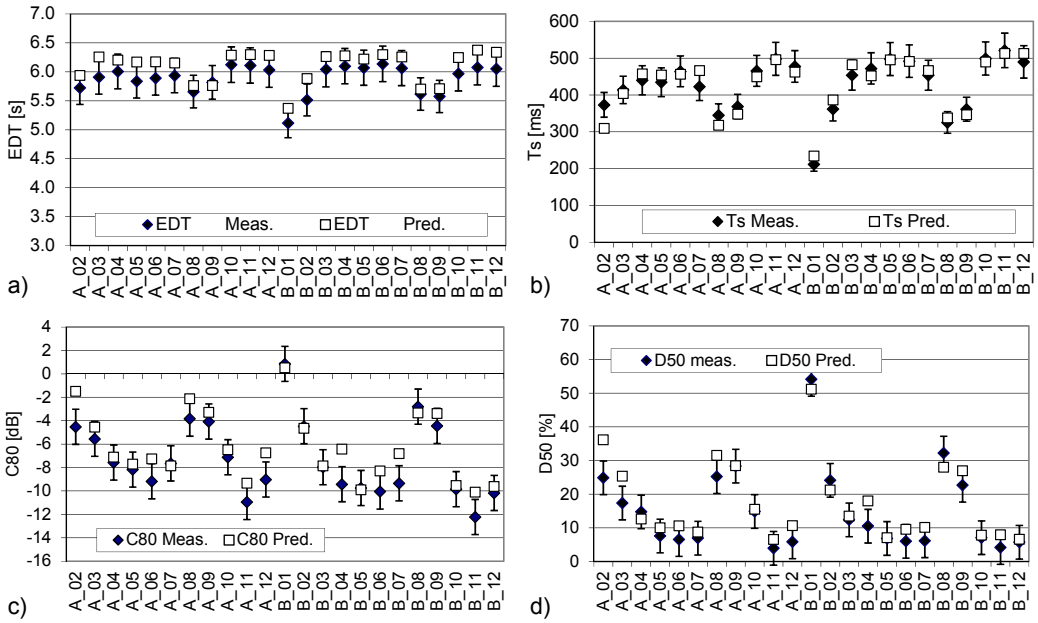


Figure 6. Measured and simulated values of early decay time (a), center time (b), clarity (c), and definition (d) averaged over mid-frequency bands (500 Hz and 1 kHZ) at each source-receiver combination in church model. Error bands represent the JND calculated as specified in ISO 3382-1 (2009) (for EDT and D50) and in Martellotta (2010) (for C80 and Ts).

0.036, 0.046, 0.054, and 0.066 in the case of the reverberant chamber, and 0.048, 0.049, 0.058, and 0.072 in the church model, the resulting absorption coefficients after the calibration ($\alpha_C$) showed largely negligible differences. In fact they ranged from 125 Hz to 1 kHz, 0.035, 0.045, 0.053, 0.065 in the case of reverberant chamber, and 0.047, 0.048, 0.056, 0.072 in the church model.

Table 3 shows the comparison between measured and simulated values of reverberation time in both models. The absolute difference between measured and predicted values was usually below 0.5 JNDs, confirming the good agreement between results over the selected octave bands.

Finally, measured values for other acoustic parameters were compared to simulated values in the CH model (the RC model was too small to provide significant variations in the acoustical parameters). The agreement was usually appropriate and the average of the absolute point-by-point variations was usually below one JND over the four frequency bands. Individual source-receiver combinations were analyzed with reference to mid-frequency averages (Figure 6). Local discrepancies between measured and simulated values appeared at times, especially for C80 and D50 which depended on direct sound and early reflections. However, the largest observed errors rarely exceeded 2.5 JNDs, even in the lowest frequency bands, while in the other cases the agreement between measured and simulated values was much better and the position-dependent variations were coherent.

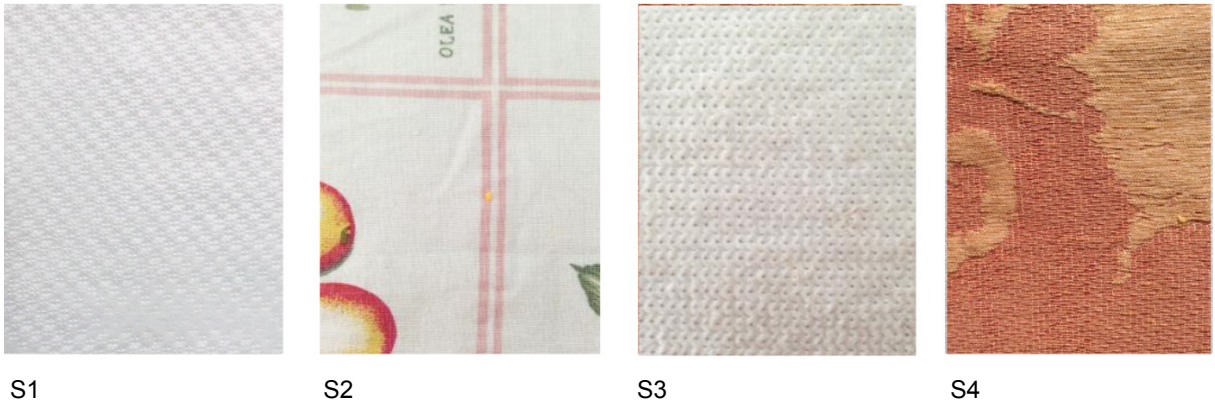


Figure 7. Detailed view of the different samples of textiles under investigation.

### 3.5. *Materials under test*

As anticipated, the search for materials capable of reproducing the acoustic properties of real scale textiles in the scaled-down models was not easy. Theoretical models showed that at high frequencies a thin layer of resistive material is likely to show nearly constant $\alpha$ and $\tau$ values. However, measured values given by Ognedal (2005) showed significant discrepancies when compared to theory. In fact, the finite dimension of hung panels is likely to affect $\alpha$ which may grow beyond the theoretical limit as diffraction around edges forces sound waves to hit the reverse of the textile, increasing the absorption. Finite thickness is also thought to have an influence and this could be particularly problematic when dealing with a 1:20 model where the equivalent full-scale thickness is greater than that expected for a thin curtain. This suggested that theoretical models could only be used as a guide to the preliminary identification of the characteristics of the materials to choose. Therefore, considering that the analysis had to be carried out over the full scale frequency range spanning from 125 Hz to 1 kHz octave bands, this corresponded to the scaled-down range from 1.7 kHz to 28 kHz. Ensuring $\alpha$ values that at 1.7 kHz are as low as those at 125 Hz would require a dramatic reduction as low as 10 g/m$^2$ in surface mass. Even assuming that such a low density could be achieved, this would also imply a significant reduction of flow resistance and hence a change in the plateau values for both $\alpha$ and $\tau$. A compromise between the different frequencies and between absorption and transmission is therefore unavoidable.

After evaluating various possibilities, four types of materials were shortlisted (Figure 7). The lightest porous material that could be found was a paper towel with a slightly bumpy surface (S1, m=20 g/m$^2$, 0.2 mm thick). The others were lightweight textile materials with different levels of open weave: a light cotton canvas (S2, m=150 g/m$^2$, 0.3 mm thick), a porous cotton fabric (S3, m=250 g/m$^2$, 2 mm thick), and a damask-fabric with an embroidered pattern (S4, m=300 g/m$^2$, 1 mm thick). For thinner materials thickness was measured by piling several layers of the same material until a readable figure was reached on the caliber. The acoustic characteristics are discussed in the next section.

## 4. Results

### 4.1. *Measured acoustic characteristics of selected materials*

Results of the measurements carried out on the selected samples are summarized in Figure 8. At this stage only measurements in the reverberant chamber were considered when deciding which materials were more suitable for the subsequent analysis. The trend as a function of frequency for the observed parameters was in line with expectations. Absorption coefficients increased as a function of frequency with a milder slope when samples were hung, while transmission coefficients

decreased, remaining substantially stable between 250 Hz and 1.25 kHz.

Material S1 had a flow resistance of 20 Pa·s/m which, combined with the low surface mass, determined its unique acoustic behavior. Absorption coefficient for the sample set on the floor remained below 0.10 up to 500 Hz, then increasing up to 0.30 at 1.25 kHz, probably thanks to the small elevations which acted as air gaps. For the hung sample $\alpha$ grew from 0.10 to 0.37 from the lowest to the highest band taken into account. Such values are compatible, although slightly higher, with those pertaining to a light tapestry such as R1 in Table 1. Coherently, $\tau$ values were the highest, with a plateau value of about 0.65.

Material S2 had a flow resistance of 90 Pa·s/m, and showed the second lowest values of sound absorption both when set on the floor and hung freely. The sample set on the floor showed a steeper increase between 500 Hz and 1 kHz, likely due to the full scale thickness of about 6 mm. The hung sample showed gently growing values reaching a maximum of 0.41 at the highest frequencies. Transmission coefficients at medium frequencies were about 0.6.

Material S3 had a flow resistance of 150 Pa·s/m, and showed the highest absorption coefficient measured with the sample on the floor. The trend as a function of frequency was more similar to that shown by thicker materials (which was no surprise, as the full scale thickness would correspond to 4 cm), or by draped curtains. In fact, the values are relatively comparable to those shown by material R4 in Table 1. Absorption coefficients measured with the sample hung free were again the highest, but the difference was not as dramatic as before, and values could be compatible with those for a heavy curtain, even though values measured by Ognedal (2005) never exceeded 0.5 in the same frequency range. Transmission coefficients showed an intermediate behavior, in reasonable agreement with values shown by heavy curtains.

Finally, material S4 had the highest flow resistance, varying between 290 and 530 Pa·s/m, depending on the portion of the sample considered. The lowest values were observed when the sample was fully embroidered, while the tighter texture of the remaining part determined the almost double values observed. Absorption coefficients were in between S2 and S3, and at mid frequencies values for the sample on the floor were higher than those of the hung sample, probably as a consequence of the thickness of the sample (equivalent to 2 cm at full scale). As expected, considering the high values of flow resistance, the transmission coefficient was the lowest, showing an average value of 0.35 in the medium frequency range.

At this point, taking into account the different characteristics shown by the selected materials, it was possible to make a first assessment of their suitability for representing real textiles. Generally speaking, the bigger differences appeared at low frequencies where, as expected, the hung samples showed systematically larger $\alpha$ and lower $\tau$ than predicted by models. However, comparisons with experimental measures given by Ognedal (2005) proved that discrepancies with theory also appeared for real scale materials, due to model limitations. The small differences in $\alpha$ between S1 and S2 and the very high $\tau$ values shown by S1, made the latter more suitable to replace a lightweight real scale textile in the subsequent analysis. Samples S3 and S4 had very different characteristics. S3 was highly sound absorbing while being sufficiently transparent, thus being probably more appropriate to represent a draped curtain rather than a textile hung straight. Conversely, S4 showed a more balanced behavior both when set on floor and hung free, with absorption and transmission coefficients which are in very good agreement with material R3 in Table 1. So, in conclusion, in order to avoid an excessive discussion of data, which in some cases were too similar to justify the use of different samples, only S1 and S4 were taken into account in the subsequent analysis. The first as a scaled-down substitute of a lightweight and transparent textile (R1), and the second to be used in place of a typical woolen textile with relatively high flow resistance (R2 and R3).

### 4.2. *Material properties derived from the geometrical acoustic model of the reverberant chamber*

Once the acoustic properties of the shortlisted materials were determined, they were used as a starting point for the subsequent modeling in GA software. However, Sabine's absorption coefficients

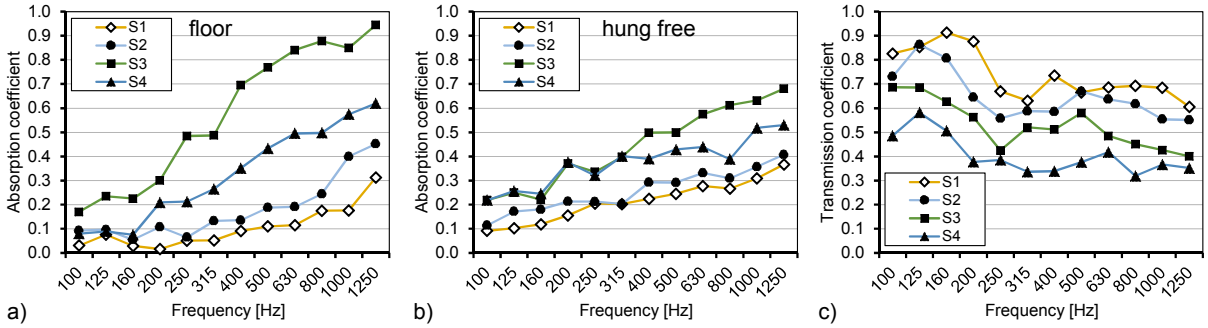


Figure 8. a) Sabine's absorption coefficients of materials under test, sample on the floor (no air gap); b) Sabine's absorption coefficients of materials under test, sample on hung free in the middle of the chamber; c) Diffuse field transmission coefficients of materials under test.

Table 4. Summary of absorption ($\alpha$) and transmission ($\tau$) coefficients of selected samples, measured (M) and derived from calibration in CATT (C), with $\tau_C$ calculated as $\tau_M/(1-\alpha_C)$. Column C,B gives the absorption coefficients derived from calibration in CATT, with samples hung in position B and assuming no transmission. Measured values were averaged over relevant 1/3 octave bands as given in Figure 8.

| | | 125 Hz | | | 250 Hz | | | 500 Hz | | | 1 kHz | | |
|---|---|---|---|---|---|---|---|---|---|---|---|---|---|
| ID | Par. | M | C | C,B | M | C | C,B | M | C | C,B | M | C | C,B |
| S1 hung | $\alpha$ | 0.10 | 0.09 | 0.13 | 0.19 | 0.16 | 0.22 | 0.25 | 0.22 | 0.33 | 0.31 | 0.30 | 0.46 |
| | $\tau$ | 0.86 | 0.96 | - | 0.73 | 0.89 | - | 0.70 | 0.93 | - | 0.66 | 0.96 | - |
| S4 hung | $\alpha$ | 0.24 | 0.23 | 0.30 | 0.37 | 0.34 | 0.46 | 0.42 | 0.40 | 0.50 | 0.48 | 0.44 | 0.66 |
| | $\tau$ | 0.52 | 0.69 | - | 0.37 | 0.58 | - | 0.38 | 0.65 | - | 0.35 | 0.66 | - |
| S1 floor | $\alpha$ | 0.04 | 0.02 | - | 0.04 | 0.08 | - | 0.11 | 0.15 | - | 0.22 | 0.45 | - |
| S4 floor | $\alpha$ | 0.08 | 0.12 | - | 0.23 | 0.25 | - | 0.43 | 0.43 | - | 0.56 | 0.65 | - |

are not the same as the statistical absorption coefficients used by simulation tools. In addition, the sound field in a chamber may not be as diffuse as necessary after a highly absorbing sample is added, thus making the application of Sabine's formula theoretically incorrect. Consequently, a convenient, and theoretically sound, way to determine absorption coefficients is to derive them from a GA model of a reverberant chamber (Benedetto and Spagnolo 1984; Summers 2003). The values determined in this way could be safely used in other GA models, without any additional adjustment.

A comparison of the values in Table 4 shows that, in general, values measured in the reverberant chamber according to Sabine's formula $\alpha_M$ were larger than the corresponding values derived from CATT-Acoustics $\alpha_C$. In most cases the differences were negligible, with the largest variations observed at high frequencies, where measured values were about 0.05 higher than simulated values. If transmission through samples was excluded, no significant variation was observed at this stage, as the sound field was sufficiently diffuse and samples were small enough to let sound move freely around them.

In order to better understand the role of transmission coefficients in GA model, a further test was carried out by placing the sample in a different position (named B in Fig. 5). This time the sample obstructed most of the cross section of the room (although a small space of about 30 cm was left open around three edges), so that most of the room volume was subdivided into two parts. In this way, if transmission was neglected, the two parts of the room were only coupled through minor openings. As expected, the results (given in columns C,B in Table 4), were significantly different under these conditions, and absorption coefficients resulting from the GA model calibration were higher than those obtained before. It is likely that this was a consequence of the negligible contribution from the less exposed face, and of the reduction in actual room volume. This confirmed, consequently, that taking into account transmission is mandatory when textile materials are used to close sub-volumes of the same space.

Absorption coefficients were then measured for the samples on the floor and the results from

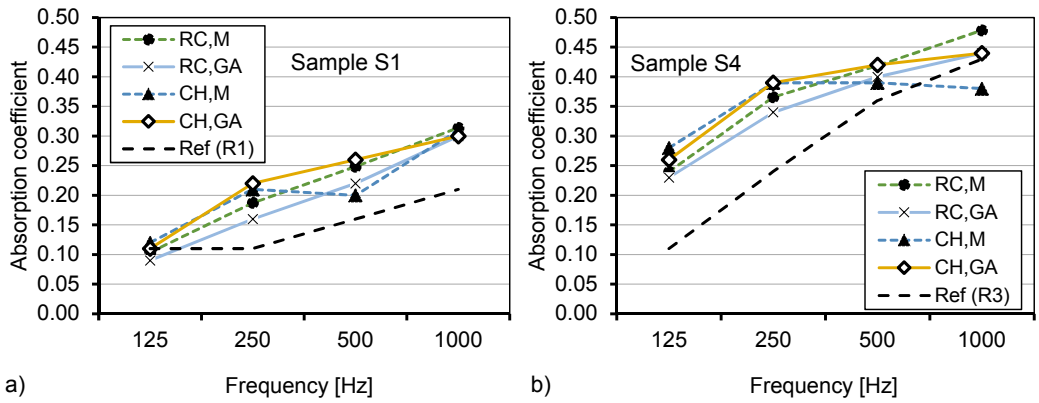


Figure 9. Absorption coefficients of selected materials hung free and measured under different conditions. a) Sample S1; b) Sample S4. RC,M = measured in reverberant chamber; RC,GA = simulated in GA model of reverberant chamber; CH,M = measured in church; CH,GA = simulated in GA model of church; Ref = reference values as given in Table 1.

125 Hz to 500 Hz showed absolute differences not exceeding 0.04 (although for S1 this resulted in much larger relative variations due to the small reference values). Conversely, at 1 kHz values obtained from the GA model showed significantly larger absolute difference (for S1 it exceeded 0.2). A possible explanation for this behavior may be found in the position of the sample which, contrary to the hung free case, does not contribute to increasing sound diffusion. Thus, slowly decaying paths might well develop far from the sample surface. As expected from the theory, these values significantly differ from those of the hung sample, as they are lower at low frequencies and rapidly increase at high frequencies.

### 4.3. *Inclusion of textiles in the church models*

Once the materials were completely characterized in the scaled-down and computerized RC models, the selected samples were applied to the CH model, in order to investigate both material behavior under different propagation conditions and the effect of material addition on church acoustics. In order to have a straightforward comparison with simulation results, measurements were carried out in 1/1 octave bands. The amount of material used was different, depending on availability, and in order to determine a significant variation in reverberation time and represent a more realistic set-up. As shown in Fig. 5, samples were hung between the arches dividing the nave from the aisles, replicating the set-up used in Fig. 1. For S1 a full scale area of 164 $m^2$ was used, while for S4 the area was 144 $m^2$. In both cases the effective area was actually doubled due to the contribution of both faces.

Under these conditions absorption coefficients of selected samples were recalculated using octave band T20 values and, as shown in Fig. 9, they were in fairly good agreement with the values determined previously. Slightly larger discrepancies appeared in the 1 kHz band for sample S4, where differences between measured values were about 0.10. Such variations are not unusual when $\alpha_S$ values are calculated, as demonstrated by Wittstock (2014). However, for sample S4 they may have been emphasized by the difference in calculation method that derived from an average over 1/3 octave bands in the RC, while in the CH it was simply based on octave band measurements. In fact, the highest frequencies were less energetic in the CH, so the resulting T20 were more influenced by the 800 Hz band (which had a lower absorption, as shown in Fig. 8).

Similarly, samples S1 and S4 were then included in the GA model of the church and their absorption coefficients redetermined. At the end of the iterative optimization procedure, the resulting absorption coefficients were those given in Fig. 9. For both materials the larger differences appeared at 250 Hz, where the maximum variation was 0.06 for S1 and 0.05 for S4. However, at the other frequencies, and at 1 kHz in particular, agreement was better. In both cases the extent of the

Table 5. Mean absolute JND error between measured and predicted values of selected acoustic parameters in the CH model after addition of samples of S1 and S4 material. O = after optimization of absorption coefficients; H = using absorption coefficients derived from the GA model of the reverberant chamber with sample hung; F = using absorption coefficients derived from GA model of the reverberant chamber with sample on the floor.

| Parameter | 125 Hz | | | 250 Hz | | | 500 Hz | | | 1000 Hz | | | average | | |
|---|---|---|---|---|---|---|---|---|---|---|---|---|---|---|---|
| | O | H | F | O | H | F | O | H | F | O | H | F | O | H | F |
| *Sample S1* | | | | | | | | | | | | | | | |
| T20 [s] | 0.8 | 0.9 | 2.0 | 0.7 | 0.8 | 2.2 | 0.8 | 0.3 | 0.9 | 0.4 | 0.4 | 1.0 | 0.7 | 0.6 | 1.5 |
| EDT [s] | 1.3 | 1.4 | 2.5 | 0.8 | 1.1 | 2.3 | 1.0 | 1.6 | 2.6 | 0.7 | 0.8 | 0.6 | 1.0 | 1.2 | 2.0 |
| C80 [dB] | 1.2 | 1.2 | 1.2 | 1.2 | 1.3 | 1.6 | 1.3 | 1.4 | 1.7 | 0.7 | 0.8 | 0.8 | 1.1 | 1.2 | 1.3 |
| D50 [%] | 0.8 | 0.8 | 0.8 | 0.8 | 1.0 | 1.1 | 1.4 | 1.5 | 1.7 | 1.4 | 1.0 | 1.1 | 1.1 | 1.1 | 1.2 |
| Ts [ms] | 1.1 | 1.1 | 1.2 | 1.4 | 2.0 | 2.9 | 1.7 | 2.2 | 2.9 | 0.9 | 0.8 | 0.9 | 1.3 | 1.5 | 2.0 |
| *Sample S4* | | | | | | | | | | | | | | | |
| T20 [s] | 1.0 | 1.1 | 2.2 | 0.5 | 0.7 | 1.9 | 0.3 | 0.4 | 0.4 | 0.5 | 0.5 | 1.4 | 0.6 | 0.7 | 1.5 |
| EDT [s] | 2.1 | 2.5 | 3.9 | 1.2 | 1.5 | 2.4 | 1.0 | 1.2 | 0.9 | 0.8 | 0.7 | 1.2 | 1.3 | 1.5 | 2.1 |
| C80 [dB] | 1.6 | 1.5 | 1.4 | 1.6 | 1.5 | 1.5 | 1.0 | 1.1 | 1.0 | 1.0 | 1.1 | 1.2 | 1.3 | 1.3 | 1.3 |
| D50 [%] | 1.5 | 1.4 | 1.3 | 1.3 | 1.3 | 1.3 | 0.9 | 1.1 | 0.9 | 0.8 | 1.0 | 1.2 | 1.1 | 1.2 | 1.2 |
| Ts [ms] | 1.3 | 1.4 | 2.1 | 1.2 | 1.4 | 2.1 | 0.9 | 1.1 | 1.9 | 1.0 | 1.1 | 1.6 | 1.1 | 1.3 | 1.9 |

variations observed seemed compatible with the standard deviation of reproducibility shown by Wittstock (2014). Considering that, as shown by Müller-Trapet and Vorländer (2015), the spatial variation of measured reverberation times is the main source of uncertainty in absorption coefficient measurements and that the latter can be expressed as a function of the ratio between room volume and sample surface, as well as of the number of source-receiver combinations and of the measured reverberation times, it can be realistically considered that such values can be applied to scale model measurements, provided that ISO 354 specifications are followed.

If transmission was neglected in the CH model, the resulting absorption coefficients remained mostly the same, probably because the samples covered only a fraction of each opening, and thus sound could freely move from one sub-volume to the other, independent of material transparency. This suggested that the role of transmission may be less critical when material is not used to close volumes, provided that the correct absorption coefficients are previously determined.

To confirm that calibration of the GA model of church with added textiles was successful, a point by point comparison of the main monaural parameters was carried out. The averages of absolute errors expressed as JND were given in Table 5 and show that, with few exceptions, good agreement was obtained. Considering that the optimization procedure was mostly based on T20 usage the corresponding JNDs were observed to be well below 1.0. Other acoustic parameters with a marked dependence on source-receiver placement showed higher JND values, particularly at low frequencies, where the agreement normally tends to be lower and, in addition, use of early-to-late energy rations can also be questionable. Large variations in a few points were usually responsible for these values. At medium frequencies the agreement was usually much better as demonstrated by the lower JND figures. For sample S1 slightly higher errors appeared at 500 Hz where receivers 03, 05, and 07 showed an increased early energy in measured parameters, probably as a consequence of some sort of pressure addition that could not be accounted for in the GA model. However, when mid frequencies were averaged, Figure 10 shows that such anomalies were evened out and the agreement was generally good. Predicted values followed the variations of the measured parameters quite accurately, with individual discrepancies rarely approaching 2.5 JNDs.

One question that could be legitimate at this point is what would happen to GA models if absorption coefficients derived from the GA,RC model were used in place of those derived from optimization. The relatively small difference between the absorption coefficients suggested that variations in objective parameters should also be small. Values given in Table 5 confirmed this for both samples. In general most of the average values showed an increase (and in a few cases slight improvements appeared), but no dramatic variation appeared in any case. The same conclusions, with even smaller variations, could be drawn if RC,M values were used (not shown in the Table for the sake of brevity). In fact, as shown in Fig. 9 the differences between absorption coefficients rarely exceed 10%, resulting in negligible effects on acoustical parameters.

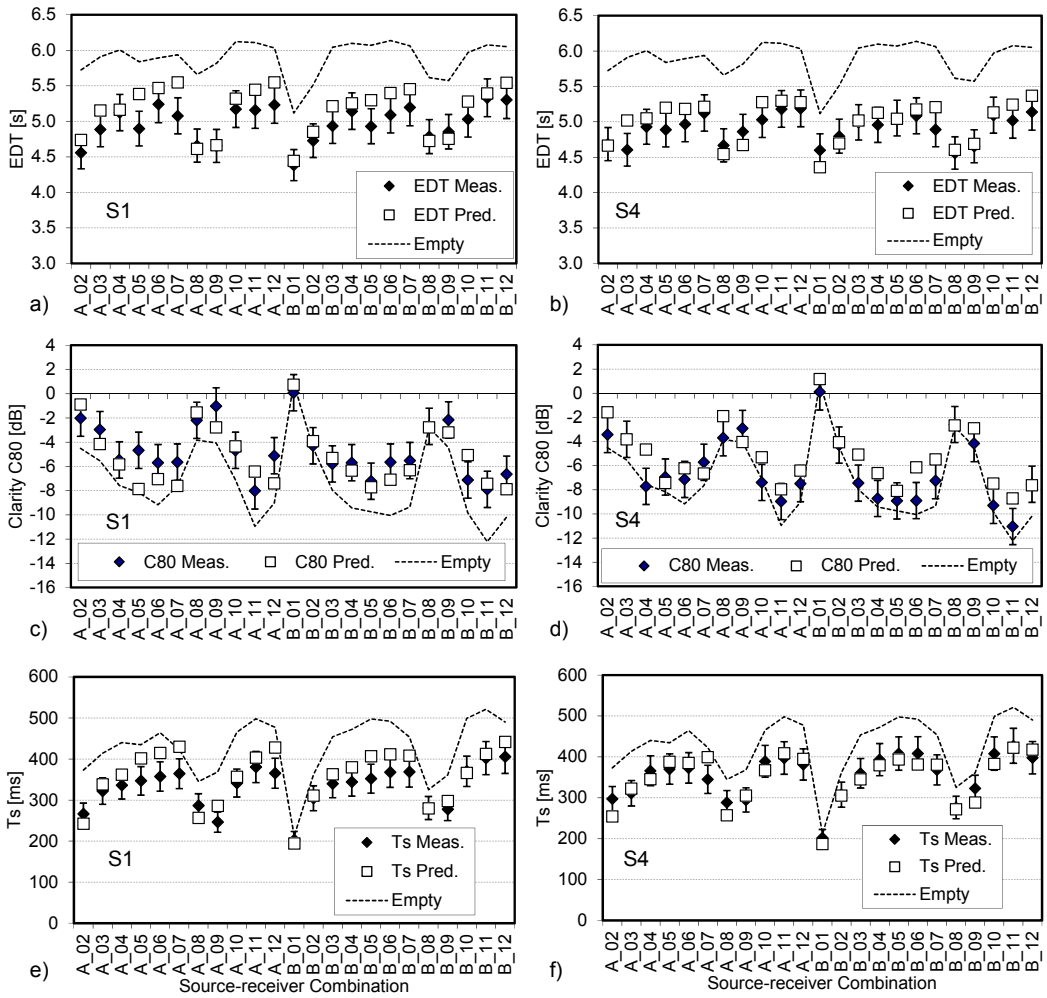


Figure 10. Measured and predicted values of EDT, C80, and Ts, averaged over mid-frequency bands (500 Hz–1 kHz) at each source-receiver combination in church model with the samples S1 (a,c,e) and S4 (b,d,f) hung below the arches. Error bands represent the JND calculated as specified in ISO 3382-1 (2009) and in Martellotta (2010).

Finally, the effect of use of absorption coefficients measured with samples on floor in place of values corresponding to samples hung free was investigated. Absorption coefficients derived from the GA model of the RC were assigned to textile surfaces, and calculations were repeated. The results in Table 5 confirmed that average errors were often doubled particularly at low frequencies and for parameters strongly influenced by the reverberant tail (T20, EDT, and Ts). Conversely, at higher frequencies the difference was not so evident, mostly as a consequence of the similarity in $\alpha$ values.

Therefore, the above results suggest that, when dealing with textiles hung freely, absorption and transmission coefficients need to be correctly measured or, at least, estimated taking into account the physical properties of the textile (surface mass and flow resistance). Use of values obtained from samples close to walls may result in significant prediction errors. The role of transmission of textile materials in the CH model was less dramatic compared to the RC. In fact, as already seen in the discussion of absorption coefficients, turning off surface transparency had relatively minor effects on the other acoustic parameters, probably because samples were mostly located in the higher part of the church and consequently had no major impact on early reflections. In addition, as already explained, they covered only a fraction of the whole opening, thus causing limited impact on diffuse field sound.

Table 6. Mean measured (M) and simulated (S) values of acoustic parameters in CH model under reference conditions (Ref) and with samples S1 and S4. Acoustic parameters are averaged over all source-receiver combinations and over the 500 Hz and 1 kHz octave bands.

| Data | Model | T30 [s] | EDT [s] | C80 [dB] | D50 [%] | Ts [ms] |
|---|---|---|---|---|---|---|
| M | Ref | 5.99 | 5.89 | -7.3 | 15.1 | 434 |
| | S1 | 5.12 | 4.97 | -4.7 | 21.1 | 333 |
| | S4 | 4.86 | 4.91 | -6.3 | 16.5 | 357 |
| | JND Ref vs S1 | 2.9 | 3.1 | 1.7 | 1.2 | 2.7 |
| | JND Ref vs S4 | 3.8 | 3.3 | 0.7 | 0.3 | 2.1 |
| S | Ref | 5.98 | 6.10 | -6.2 | 17.6 | 430 |
| | S1 | 4.88 | 5.00 | -4.9 | 20.8 | 346 |
| | S4 | 4.84 | 5.00 | -5.2 | 19.2 | 352 |
| | JND Ref vs S1 | 3.7 | 3.6 | 0.9 | 0.6 | 2.3 |
| | JND Ref vs S4 | 3.8 | 3.6 | 0.7 | 0.3 | 2.1 |

### 4.4. *The effect of textiles on church acoustics*

Finally, the collected results were used to briefly comment on the effect that textile addition may have on church acoustics. The discussion aimed to show the magnitude of variations in acoustic parameters to be expected following the installation of textiles in a church. However, the church under investigation was an idealized model and the quantity and positioning of textiles was realistic, but nonetheless arbitrary and aimed at investigating the effect of one single material at a time, while historical research summarized in the introduction suggests that combinations of different materials were more likely. Nonetheless, a comparison with the reference conditions may shed some light on the expected effect of tapestries and textiles in churches.

To provide a reference, the dashed line in Figure 10 recalls the corresponding values of each parameter measured in the empty model. Comparisons between measured parameters were carried out to overcome any possible limitation of the simulations. However, comparisons between GA models (empty and with samples in them) actually provided comparable variations (Table 6). No major differences appeared between S1 and S4, because the higher absorption coefficients for S4 were compensated for the larger sample area for S1. The differences were greater for reverberation times (both T20 and EDT), where differences between 2.9 and 3.8 JNDs appeared at mid-frequencies. Center time was consequently affected by the reverberation time variation and showed variations between 2.1 and 2.7 JNDs. Almost surprisingly, early-to-late energy ratios showed comparatively smaller changes, varying between 1.2 and 1.7 JNDs for S1 and between 0.3 and 0.7 for S4. Analysis of point-by-point variations in Figure 10 confirmed that S4 variations in C80 due to sample addition had no audible effect. An explanation for this behavior can be found in the elevated position of the samples which had little influence on the reflection paths contributing to the stronger reflections, and resulting in a small change in their ratio. All the other parameters, more influenced by late reverberant sound, showed bigger changes but the position-dependent trend remained the same between the reference and the set-up conditions. To confirm the importance of direct sound and early reflections, receivers close to the source showed smaller variations than those located further away. Finally, the variation as a function of frequency showed lower impact in the lower bands, but this was expected as a consequence of the lower sound absorption of materials in that part of the spectrum.

From the listener perspective the addition of textiles brought about a notable reduction in reverberation time (probably not so dramatic under fully occupied conditions), and a slight increase in clarity. The latter parameter could be further improved by moving the sound absorbing elements closer to the audience.

## 5. Conclusions

This paper addressed the complex topic of the simulation of free hung textiles in geometrical acoustic simulation tools. As one of the problems was the lack of experimental data referring to this configuration and their subsequent application to real spaces, the research relied on scale model measurements that reproduced all the different steps. In particular, a reverberant chamber and a basilica plan church were used as references.

Firstly, the general characteristics of textile materials were outlined and the theoretical models used to describe their acoustic behavior were briefly summarized. Theoretical predictions of absorption coefficients under different mounting conditions were determined to clarify that sound absorption of samples close to walls may yield clearly incorrect results if used for free hung samples.

Suitable materials were first identified to represent textiles in scaled-down models. After measuring their acoustic properties, including sound absorption, transmission coefficients, and flow resistance, two samples were selected for the subsequent analysis. These represented a lightweight textile with high transmission and a more conventional woolen curtain with lower transmission.

The sound absorption coefficients were then optimized for use in geometrical acoustic simulations through their iterative adjustment and matching of reverberation times. Initially, the case of the reverberant chamber was analyzed. For samples hung free small variations appeared, with $\alpha_{\mathrm{C}}$ values lower than $\alpha_{\mathrm{M}}$ values, and a maximum difference of 0.04 appearing in a couple of cases. If samples were hung in the center of the room and large spaces were left around them $\alpha_{\mathrm{C}}$ were the same with or without transmission through sample. However, if the sample was larger and placed in a way that isolated a part of the volume (with limited opening surface between sub-volumes), things changed significantly. If transmission was neglected $\alpha_{\mathrm{C}}$ values were systematically higher, up to 0.22 in absolute value and with relative variations usually around 50%. Conversely, if transmission was included, resulting $\alpha_{\mathrm{C}}$ values showed no change. This confirmed the importance of taking acoustic transparency into account when a sample is used to close parts of a volume.

Finally, the selected samples were hung free in a scale model of a church and measurements were compared with geometrical acoustic simulation following the usual optimization. Measured absorption coefficients showed only small differences in comparison with reverberant chamber data, and values derived from GA model showed similar variations. This implied that direct use absorption coefficients obtained in reverberant chamber (either scaled down or GA model, provided that transparency was taken into account) yielded fairly accurate predictions of most acoustic parameters with errors that, on average, were within 1 JND at mid frequencies. The effect of transparency was negligible in this case as the samples could not fully divide sub-spaces.

The effect of textiles on church acoustics proved to be more evident at medium frequencies than at low frequencies, as was to be expected considering sound absorption coefficients. Reverberation times and center time were affected most, while early-to-late energy ratios showed smaller variations, probably as a result of placing the material in a position which did not affect the stronger reflections.

In conclusion, GA models were able to take into account the effect of textile materials with reliable accuracy provided that input data were correctly determined. Transmission played an important role in the determination of absorption coefficients to use in GA models, and in all the cases in which the textile material subdivided the original space into sub-volumes. Further investigation is advised in order to characterize absorption and transmission coefficients of textile materials on a real scale to further confirm the above findings.

## Acknowledgements

This work has been partially funded by the Spanish Ministry of Science and Innovation and FEDER funds, with references PatrimoniUN10 CEI 2014/731 and BIA2014-56755-P. One of the authors (A. Alonso) received an FPU grant from the Spanish Government (ref. FPU12/04949). The authors

are finally grateful to the anonymous reviewers for their constructive criticism and suggestions for the improvement of the manuscript.

## References

Alonso A., Sendra J.J., Suárez R., Zamarreño T. 2014, "Acoustic evaluation of the cathedral of Seville as a concert hall and proposals for improving the acoustic quality perceived by listeners" *Journal of Building Performance Simulation* 7 (5): 360–378.

Astolfi G., Garai M, Secchi S, 2000, "Scale model investigation on the influence of boundary conditions on the airborne sound insulation of lightweight double walls", *J. Building Acoust.* 7(4): 263–276.

Barron, M. 1983, "Auditorium acoustic modelling", *Applied Acoustics* 16: 279–290

Benedetto G., Spagnolo R. 1984, "Evaluation of sound absorbing coefficients in a reverberant room by computer-ray simulation", *Applied Acoustics* 17: 365 - 378.

Allard J.F., Champoux Y. 1992, "New empirical equations for sound propagation in rigid frame fibrous materials", *J. Acoust. Soc. Am.* 91(6):3346-3353.

Chiles S. 2004, "Sound Behaviour in proportionate Spaces and Auditoria". Doctoral Thesis, University of Bath, UK.

Christensen C.L., Koutsouris G. and Rindel J.H. 2014, "Estimating absorption of materials to match room model against existing room using a genetic algorithm", in *Proc. Fourm Acusticum 2014*, Krakow (Poland) 7-12 September 2014.

Cox T.J., D'Antonio P. 2004, "Acoustic Absorbers and Diffusers", Spon Press, UK.

Cutts E.L. 1854, "An essay on church furniture and decoration". University of Oxford, UK.

Dalenbäck B.I. 2011, "CATT-Acoustic v9 powered by TUCT, user manual". Gothenburg, Sweden.

Delany M.E., Bazley E.N. 1970, "Acoustical properties of fibrous absorbent materials", *Appl. Acoust.* 3: 105-116

del Rey R., Alba J., Arenas J.P., Ramis J. (2013), "Evaluation of Two Alternative Procedures for Measuring Airflow Resistance of Sound Absorbing Materials", *Archives of Acoustics*, 38(4): 547–554.

Farnetani A., Prodi N., Pompoli R., "On the acoustics of ancient Greek and Roman theaters", *J. Acoust. Soc. Am.* 124: 1557–1567.

Goehring M. 2009, "Shrine, Decoration, Textiles". *Encyclopedia of Medieval Pilgrimage*, edited by Larissa J. Taylor, et al.: 682-683

Hak, C.C.J.M., Wenmaekers, R.H.C., Luxemburg, L.C.J. van 2012, "Measuring Room Impulse Responses: Impact of the Decay Range on Derived Room Acoustic Parameters", *Acta acustica united with Acustica*, 98: 907 - 915

Ingard U.K. and Dear T. A. 1985, "Measurement of acoustic flow resistance", *J. Sound Vib.*, 103: 567-572.

ISO 9613-1:1993, "Acoustics Attenuation of sound during propagation outdoors Part 1: Calculation of the absorption of sound by the atmosphere", International Organization for Standardization, Geneva, Switzerland.

ISO 9053:1991, "Acoustics materials for acoustical applications. Determination of airflow resistance", International Organization for Standardization, Geneva, Switzerland.

ISO 354:2003, "Acoustics: Measurement of sound absorption in a reverberation room", International Organization for Standardization, Geneva, Switzerland.

ISO 3382-1:2009(E). "Acoustics-Measurement of room acoustic parameters, Part 1: Performance spaces", International Organization for Standardization, Geneva, Switzerland.

ISO 10140-2:2010 , "Acoustics – Laboratory measurement of sound insulation of building elements – Part 2: Measurement of airborne sound insulation", International Organization for Standardization, Geneva, Switzerland.

Jeon J.Y., Ryu J.K., Kim Y.H, Sato S. 2009, "Influence of absorption properties of materials on the accuracy of simulated acoustical measures in 1:10 scale model test". *Applied Acoustics*, 70: 615–625.

Kuttruff H. 2009, "Room acoustics", Spon Press, UK.

Leishman T.W., Rollins S., Smith H.M. 2006, An experimental evaluation of regular polyhedron loudspeakers as omnidirectional sources of sound, *J. Acoust. Soc. Am.* 120(3): 1411-1422.

Luizard P., Polack J.D., and Katz B.F.G. 2014, "Sound energy decay in coupled spaces using a parametric analytical solution of a diffusion equation", *J. Acoust. Soc. Am.* 135: 2765–2776.

Martellotta F. 2010, "The just noticeable difference of center time and clarity index in large reverberant spaces", *J. Acoust. Soc. Am.* 128: 654–663.

Martellotta F. and Castiglione M.L. 2011, "On the use of paintings and tapestries as sound absorbing materials", In Proc. *Forum Acusticum 2011*, 27 june-1 july 2011, Aalborg (DK), Paper 00078.

Martellotta F. 2013, "Optimizing stepwise rotation of dodecahedron sound source to improve the accuracy of room acoustic measure", *J. Acoust. Soc. Am.*, 134(3): 2037–2048

Müller-Trapet M., and Vorländer M. 2015, "Uncertainty analysis of standardized measurements of random-incidence absorption and scattering coefficients", *J. Acoust. Soc. Am.*, 137(1): 63–74

Ognedal M. 2005, "Sound absorption in freely suspended textile banners,"MSc thesis, NTNU, Dept. of Civil and Transport Eng., Trondheim, Norway.

Pelzer S., Vorländer M. 2013, "Inversion of a room acoustics model for the determination of acoustical surface properties in enclosed spaces", *Proc. Meeting on Acoustics*, 19, 015115.

Polack J.D., Meynial X., Grillon V. 1993, "Auralization in scale models: Processing of impulse response", *J. Audio Eng. Soc.*, 41(11): 939-945.

Rebillard P., Allard J.-F., Depollier C., Guignouard P., Lauriks W., Verhaegen C., Cops A. 1992, "The effect of a porous facing on the impedance and the absorption coefficient of a layer of porous material". *J. Sound Vib.*, 156: 541-555.

Ryu J.K., Jeon J.K. 2008, "Subjetive and objective evaluations of a scattered sound field in a scale model opera house". *J. Acoust. Soc. Am.*, 124(3): 1538–1549.

Santos-Gómez S. San Andrés-Moya M. 2004, "La pintura de Sargas", *Archivo Español de Arte* 77(305): 59–74.

Schnoebelen A. 1969, "Performance practices at San Petronio in the baroque", *Acta Musicologica* 41(1/2): 37–55.

Simons M.W. 1982, "The measurement of Airborne Sound Insulation using Acoustic Scale Models", *Architectural Science review* 25(1): 10–15.

Soeta Y., Ito K., Shimokura R., Sato S., Ohsawa T., Ando Y. 2011, "Effects of sound source location and direction on acoustic parameters in Japanese churches", *J. Acoust. Soc. Am.* 131(2): 1206–1220.

Summers J.E. 2003, "Measurement of audience seat absorption for use in geometrical acoustics software". *Acoustic Research Letters Online*, 4(3): 77–82.

Summers J.E., Torres R.R., Shimizu Y., and Dalenbäck B.I. 2005, "Adapting a randomized beam-axis-tracing algorithm to modelling of coupled rooms via late-part ray tracing", *J. Acoust. Soc. Am.* 118: 1491-1502.

Vorlander M. 2008, "Auralization", Springer verlag, Germany.

Weigert L. 2004, "Weaving Sacred Stories: French Choir Tapestries And The Performance Of Clerical Identity". Cornell University Press.

Wenmaekers R.H.C, Hak C.C.J.M, Hornikx M.C.J., 2014, "The effective air absorption coefficient for predictibg reverberation time in full octave bands", *J. Acoust. Soc. Am.*, 136(6): 3063–3071.

Wittstock W., "Uncertainties for the determination of the absorption coefficient according to ISO 354", In Proc. *Forum Acusticum 2011*, 27 june-1 july 2011, Aalborg (DK).